SEMARAK ILMU PUBLISHING

Journal of Advanced Research in Fluid Mechanics and Thermal Sciences

Journal homepage:
https://semarakilmu.com.my/journals/index.php/fluid_mechanics_thermal_sciences/index
ISSN: 2289-7879

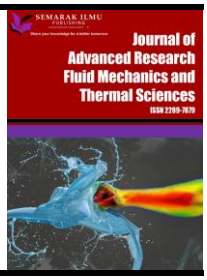

Modelling Analysis and Characteristics of Multi-Level Inverter for Integrating Solar PV System to Grid

Anil Kumar Rai[1], Arun Kumar Maurya[1,*], Ritesh Kumar Sharma[1], Mansi Singh[1]

[1] Electrical and Electronics Engineering Department, Ajay Kumar Garg Engineering College, Ghaziabad, Uttar Pradesh-201015, India

ARTICLE INFO

Article history:
Received 18 August 2024
Received in revised form 30 November 2024
Accepted 9 December 2024
Available online 20 December 2024

Keywords:
Solar power generation; tracking the highest power output; multi-level inverter; total harmonics distortion

ABSTRACT

This paper investigates the implementation of a cascaded H-bridge multi-level inverter in a single-phase grid-connected solar photovoltaic (PV) system to address harmonic distortion challenges in DC-to-AC power conversion. The primary objective is to enhance power quality and system efficiency by leveraging the inverter's ability to reduce harmonics through power sharing and a lower switching frequency. A Simulink model is developed to evaluate the proposed system's performance, incorporating a unipolar Pulse Width Modulation (PWM) control strategy and an LCL filter for effective harmonic mitigation. The system employs Maximum Power Point Tracking (MPPT) based on the Perturb and Observe (P&O) algorithm, combined with Synchronous Reference Frame Theory-Phase Disposition PWM (SRFT-PDPWM) for optimal control. The proposed inverter ensures precise synchronization between the grid and inverter frequencies, achieving a Total Harmonic Distortion (THD) below 5%. Simulation results demonstrate the system's robust responsiveness to variations in solar irradiance, with increased irradiance leading to further reductions in THD and improved power quality. These findings validate the proposed inverter's capability to deliver high-quality, efficient power under varying environmental conditions, aligning with global objectives for integrating clean and sustainable energy into utility networks.

1. Introduction

Solar PV system generates power with zero carbon emission and UN mission's objective is to enhance the adoption of grid-connected PV systems capable of exporting power to utility networks, thus contributing to global energy needs without relying on fossil fuels. One significant challenge to address is the enhancement of power quality. Multilevel Inverters offer a solution to this challenge. Over 90% of loads exhibit inductive characteristics, resulting in harmonics that are either integer or non-integer multiples of the fundamental frequency. The grid fed voltage/current waveform can be almost sinusoidal by using the multi-level inverter and grid frequency should be matched with the frequency of signal that is being injected into grid. The current-voltage characteristics of solar PV array is non-linear in nature and depends on the unpredictable incident solar radiation and ambient

* *Corresponding author.*
E-mail address: arunupscee@gmail.com

https://doi.org/10.37934/arfmts.125.2.8292

temperature. The MPPT controller used in PV system tends to be also non-linear and time varying. Several MPPT techniques have been proposed and developed with varying degree of complexity, design and cost [1]. Grid-connected PV systems have generally two control loops. The pulse width modulated inner loop modulates the inverter current output to meet the phase and waveform requirements whereas outer loop decides the inverter power output according to the maximum power point of the solar PV array. Both the loops are realized simultaneously with a control approach rooted in Synchronous Reference Frame Theory-Phase Disposition Pulse Width Modulation (SRFT-PDPWM) combined with the Perturb and Observe (P&O) Maximum Power Point Tracking (MPPT) technique.

2. System Configuration

The basic structure of the proposed grid-connected solar PV system consists of PV array, DC-DC converter, a multi-level inverter, MPPT controller and filter as shown in Figure 1. In the proposed grid connected solar photovoltaic system, PV array of capacity 5 kWp, use the P&O algorithm to keep the operational point of the array at Maximum Power (MPP), which injects high sinusoidal current into the grid. A 3-level cascaded H-bridge inverter with inductor-capacitor-inductor (LCL) filter have been considered.

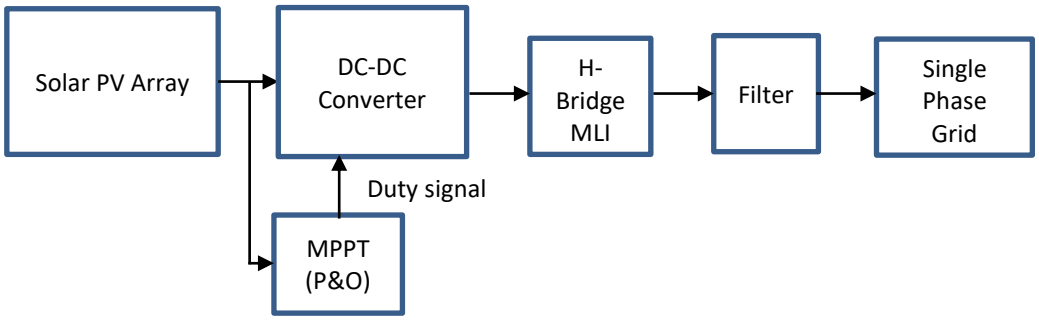

Fig. 1. The proposed system's structure

3. System Modelling

3.1 Solar PV Array

In real-world situations, the solar PV array is configured using a suitable combination of series and parallel connections of solar PV modules to align with the necessary current and voltage specifications during standard operation. The photo-generated current (Iph) is contingent upon both the level of sunlight (insolation) and the temperature, and its expression is provided by Aryal *et al.,* [2].

$$I_{ph} = \frac{G}{G_{ref}}\left(I_{ph,ref} + I_{scc}\left(\left(T_c - T_{c,ref}\right)\right)\right) \quad (1)$$

Here, G and Gref stand for the real and specified solar radiation levels (measured in W/m2), while Tc and Tc, ref represent the current and specified operating temperatures of the cell (measured in Kelvin). Iscc corresponds to the temperature coefficient of the short circuit current as provided by the manufacturer (measured in A/K).

The diode current is given by Shockley equation

$$I_D = I_0 \left(exp \left[\frac{q(V+IR_S)}{mkT_c} \right] - 1 \right) \quad (2)$$

In this context, Vc represents the voltage across the diode (measured in volts), I_0 denotes the reverse saturation current (measured in amperes), η stands for the diode ideality factor, Rs signifies the series resistance (measured in ohms), e represents the charge of an electron (1.602 x 10^-19 C), and K represents the Boltzmann constant (1.38 x 10^-23 J/K).
The reverse saturation (I_0) current is given by [3]

$$I_0 = I_{0,ref} (\frac{Tc}{Tc,ref})^3 exp \left[\left(\frac{eE_g}{\eta K} \right) \left(\frac{1}{Tc,ref} - \frac{1}{Tc} \right) \right] \quad (3)$$

whereas the shunt current, I_{sh} is given by

$$Ish = \frac{Vc}{Rp} \quad (4)$$

R_p is the shunt resistance (Ω).

The above Eq. (1) can be written as

$$I = I_{ph} - I_0 \left(exp \left[\frac{q(V+IR_S)}{mkT_c} \right] - 1 \right) - \frac{(V+IR_S)}{R_{sh}} \quad (5)$$

In terms of voltage, the above equation can be written as

$$V = N_s \lambda \ln \left(\frac{I_{ph} - I + N_p I_0}{N_p I_0} \right) - \frac{N_s}{N_p} R_s I \quad (6)$$

And $\lambda = \frac{\eta K T_c}{e}$, where Ns is the number of modules connected in series and Np is the number of such series connected module in parallel.

For the proposed work, solar PV array consists of each module of capacity 270 Wp made of AVID-SOLAR-ASMS. The details of the module are as follows in Table 1:

Table 1
The details of the solar PV module

Solar PV modules	6×3
P_{max}	270Wp
Open circuit voltage (V_{oc})	44.5 V
Short Circuit current (I_{sc})	8.42 A
Current at Maximum power (I_{mp})	7.69 A
Voltage at Maximum power (V_{mp})	35.1 V
Fill-factor	0.72
Series string (Ns)	6
Parallel string (Np)	3

Thus, for given PV array the current and voltage at MPP are 210.6 V and 23.07 A respectively. The Peak Power is 4858.542Wp.

3.2 DC-DC Boost Converter Modelling

The system includes an inductor, a MOSFET, a diode and a capacitor on the input side, along with a capacitor on the output side. Before proceeding with the modeling, several assumptions have been established:

i. Ideal behavior is assumed for the switching equipment.
ii. Equivalent series resistance is taken into account.
iii. The inductor's current operates continuously.
iv. Each and every passive element, employed in the system are considered linear, time-invariant and not dependent on frequency.

The DC-DC boost converter serves two primary objectives. Firstly, it elevates the direct current (DC) voltage level from the solar output to ensure operation at the maximum power point. Secondly, its primary function is to deliver a steady voltage output at the boost connection locations where the grid-connected H-bridge multi-level inverter has a steady supply of power. The average voltage at these boost terminals is controlled by adjusting the duty cycle which is denoted as "D." This duty cycle is determined by the gate signal applied to the switch, typically a MOSFET which is defined as the duration when the switch is turned on relative to the total switching period. The MPPT controller is responsible for defining and controlling this duty cycle. The switching process follows a pulse width modulation (PWM) scheme, operating at a specific switching frequency with defined pulse durations for both the "on" and "off" states. In this context, we have chosen a MOSFET switching frequency of 10 kHz. The single-phase voltage source inverter is supplied with a direct current (DC) voltage, as indicated by the following.

$$V_{DC} = \frac{2\sqrt{2}\,V_S}{\sqrt{3}\,m} \tag{7}$$

In this context, Vs represents the root mean square (r.m.s.) value of the input voltage, which is 200 volts. The modulation index of the inverter, typically assumed as 0.95, is represented as 'm.' When these values are applied, we calculate a resulting value of 343.78 volts.

Duty cycle of boost converter is expressed by

$$D_y = 1 - \frac{V_{in}}{V_{out}} \tag{8}$$

where ripple content in inductor current is ΔI_L and this ripple content is assumed to be 5% of the DC-DC inductor current, which amounts to 1.393 A.

The boost inductor value is given by

$$L_{DC} = \frac{V_{DC} \times D_y\,(1-D_y)}{2 \times F_{SW} \times \Delta I_L} \tag{9}$$

After substituting the values mentioned earlier into Eq. (8), we calculate an initial value of 2.48 milli-Henries (mH). However, following the optimization of the model, the value utilized in the simulation has been adjusted to 45 mH.

The capacitance value at the boost terminals, as indicated by Selvaraj and Rahim [3], is provided

as follows.

$$C_{\beta} = \frac{I_{dc}}{2\times \omega \times V_{DC(ripple)}} \tag{10}$$

Initially, the calculated value is approximately 6 µF. However, after optimization, it was determined that a value of approximately 5800 µF is the most suitable choice in accordance with the paper's requirements. Here, "C" represents the capacitance, "I_dc" is the DC current at the boost input terminals, "ω" stands for the angular frequency (2 * π * 50), and "V_r" denotes the ripple content in the output DC voltage, which is 6V. Additionally, a capacitance value of 100 µF is used to ensure a stable input DC, and a series equivalent resistance of 0.0001 Ω is included.

3.3 Selection of Filter

When compared to L or LC filters, inductor-capacitor-inductor (LCL) filters exhibit better dynamic response and damping effectiveness. The choice of the utilization of an LCL filter arises from the necessity to diminish elevated-frequency current harmonics that enter the grid while also enhancing the decoupling between the grid impedance and the filter. Nevertheless, to achieve a satisfactory response, very small values of inductance (L) are employed, leading to resonance problems and unstable system behavior. These issues predominantly address high-frequency harmonics filtration and the absorption of reactive power. Consequently, there is a need to optimize LCL filter values through parameter adjustments.

For choosing an AC Inductor at the side of the inverter, see [3]:

$$L_{Fi} = \frac{\sqrt{3}\times m \times V_{DC}}{12 \times h \times F_{SW} \times \Delta I_L} \tag{11}$$

Here, we consider the overloading factor "h," which is set to 1.2, along with a switching frequency of 10 kHz for a single-phase three-level inverter. After substituting these values into Eq. (6), we calculate an inductance value of 2.81 milli-henries (mH). The Value of inductance for Grid side inductor is given by $L_{Fg} = h * L_{Fi}$ = 1.2 times inverter side inductance.

Thus, inverter side and grid side are 80mH and 82mH respectively. The value filter capacitance is given by [3]

$$C_F = \frac{0.05}{\omega_G * Z_{base}} \tag{12}$$

where

$$Z_{base} = \frac{V_{L-L}}{P_{active}}$$

In this context, "V" represents the grid's line-to-line voltage, "P" represents the inverter's designated active power capacity, while "f" denotes the operational frequency of the grid. The resonant frequency is calculated according to Selvaraj and Rahim [3]

$$\omega_{resonant} = \sqrt{\frac{(L_{Fi} + L_{Fg})}{(L_{Fi} \times L_{Fg} \times C_F)}} \quad (13)$$

From Eq. (12), the value of resonant frequency is 2.1 kHz. Furthermore, to reduce the resonance problem a parallel damping is done with C_F and resistance, R_D required to carry out parallel damping is given by

$$R_D = \frac{1}{(3 \times \omega_{resonant} \times C_F)} \quad (14)$$

The calculated values of R_D and C_F are 500 Ω and 5 µF respectively. However, the performance of LCL filter is better if value of CF is taken as 2.2 µF in the simulation.

4. MPPT Technique

To ensure the solar PV system operates efficiently, it is essential to achieve an optimal transfer of the energy produced in the array to the load. The internal resistance of solar PV module depends on incident solar radiation and module operating temperature and hence characteristics is non-linear in nature. Various peak power tracking methods have been previously suggested, employing diverse control strategies [4-7]. Some utilized conventional proportional integral derivative (PID) controllers, while others opted for a tracking regulator based on fuzzy logic principles with associated rules [8]. and review of MPPT algorithms has been presented [9]. There is variation in the degree of intricacy, number of sensors used, convergence rate, and cost of different methods. Additionally, the equipment used in the application and its effectiveness range differ.

The maximum power will be transferred if load impedance matches the source impedance. The MPPT charge controller works in tandem with the boost converter to control the duty cycle of the converter in order to get the voltage necessary for optimizing power production. In this paper, P&O MPPT technique has been used to extract the maximum power from PV Array This approach functions on the premise that the maximum power point When the power of the solar array remains constant with respect to its voltage, the Maximum Power Point (MPP) is reached. The controller associated with this approach initially assesses whether there is a positive change in power and subsequently determines whether the voltage is rising or falling.

The controller will increase the voltage to obtain the maximum power if both the voltage change and the power change are positive. A similar process is applied to address other scenarios. Consequently, based on the prevailing conditions, the controller will adjust the voltage either upwards or downwards to track the maximum power. This iterative procedure is repeated until the MPP is attained.

This approach is known as the perturb and observe (P&O) method (flowchart as mentioned in Figure 2) and it is widely used, even though it can lead to fluctuations in power output. It is also sometimes called the hill climbing method because it relies on ascending the power curve concerning voltage up to the maximum power point (MPP) and descending beyond that point. The perturb and observe method is favored for MPPT due to its straightforward implementation.

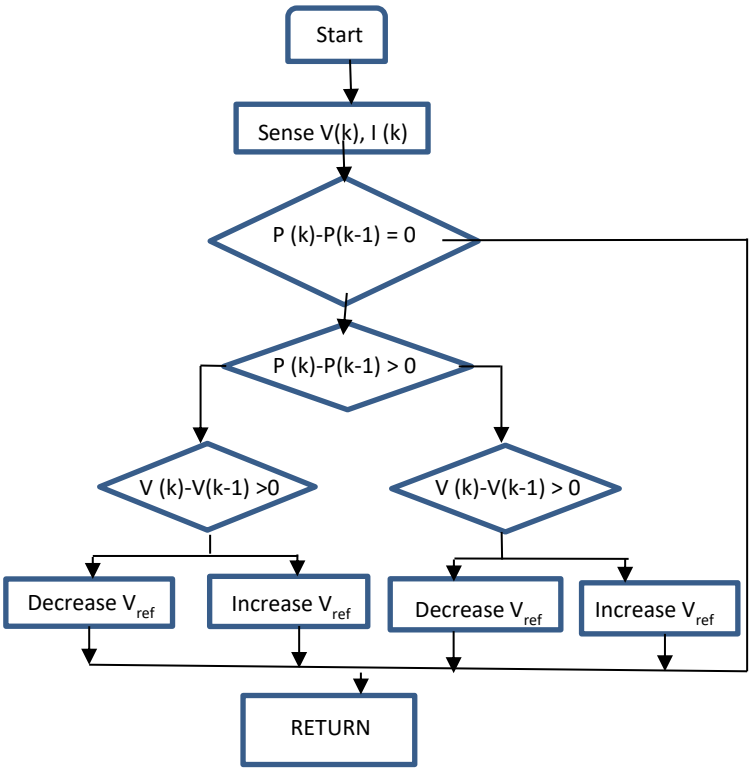

Fig. 2. Flowchart of perturb and observe algorithm

5. Control Schemes

The suggested system combines a two-stage solar grid connected configuration with multi-level inverters. Maximizing power transmission from the PV array to the load side is achieved by controlling the MOSFET's duty signal in the boost converter, which is decided by MPPT algorithms. This is accomplished during the initial DC-DC power conversion step by lining up the impedance with that on the load side and that on the source side. The DC-DC boost converter's characteristics must be carefully chosen because the H-Bridge needs a constant, uninterrupted voltage source. In the second stage, DC power is transformed to AC power, which is then sent through an LCL filter and a three-level output inverter to the 230-volt, single-phase, 50Hz grid. In section 1 Parameters of LCL filter is already discussed.

The equation $k = 2v + 1$ defines the quantity of output phase voltage levels "k" in a multilevel inverter, where "v" signifies the count of isolated DC sources connected to the input of the H-bridge or, in other words, the number of H-Bridges utilized. Each H-bridge incorporates four switches, and the gating pulse and switching pattern of the inverter's structure affect the output voltage level. When the inverter is operational, its output voltage levels include +Vdc, 0, and -Vdc. H-Bridges are constructed using IGBT/MOSFET switches with high-speed switching capabilities, and they find applications in high-power scenarios and other similar context. The schematic diagram of three level H-Bridge inverter as shown in Figure 3 [10].

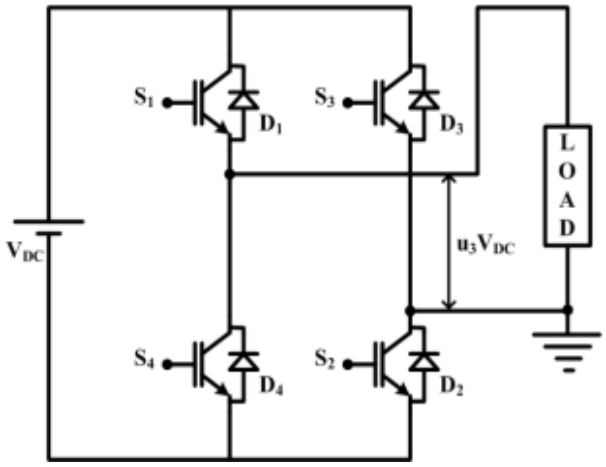

Fig. 3. Schematic diagram of 3-level H-Bridge inverter [5]

In the simulation for this paper, a 3-level cascaded H-bridge multi-level inverter is employed, and it's powered by a sinusoidal pulse width modulation (SPWM) UNIPOLAR injection technique as shown in Figure 4. Within this configuration, PWM signals serve as gate control pulses, and they are generated using a single reference signal. To replicate this modulation approach in the SIMULINK environment, a closed-loop control system is implemented [11-13].

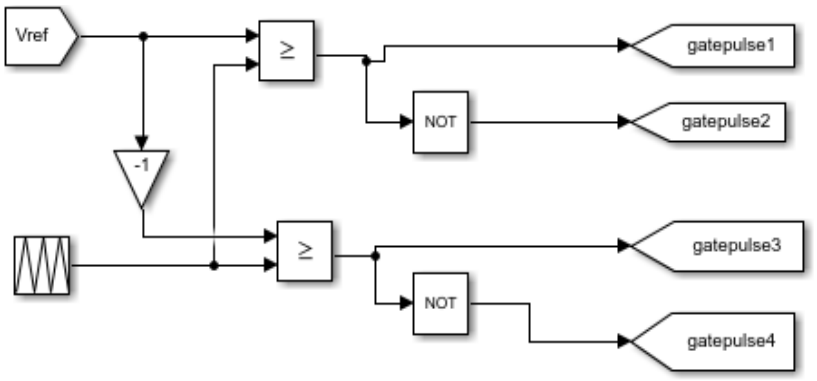

Fig. 4. The SPWM modulation technique is employed by the inverter to produce gate pulses

Within PWM control, the output voltage is fine-tuned by varying the duration of the pulses, and this adjustment occurs as the inverter switches are cyclically activated and deactivated during half a cycle. The reference or modulation waveform is positioned at the midpoint of the carrier set, featuring a peak amplitude denoted as Ar and a frequency of fr. The fundamental concept behind a carrier-based PWM method involves continuous comparison of a bus voltage output, regulated by a PI controller, with a carrier wave, typically represented as a triangular carrier wave [14,15]. The reference signal and the carrier signal are continually assessed. When the reference signal surpasses the carrier signal, the switch associated with that carrier is turned on; conversely, the switch for that carrier remains off if the reference signal is weaker than the carrier signal. Adopting this technology offers advantages in high-power applications, accommodating high voltage levels, minimizing harmonic distortions, and reducing switching losses. By simulation, we have received Phase voltage (three levels) and current waveform of the inverter output characteristics as shown in Figure 5.

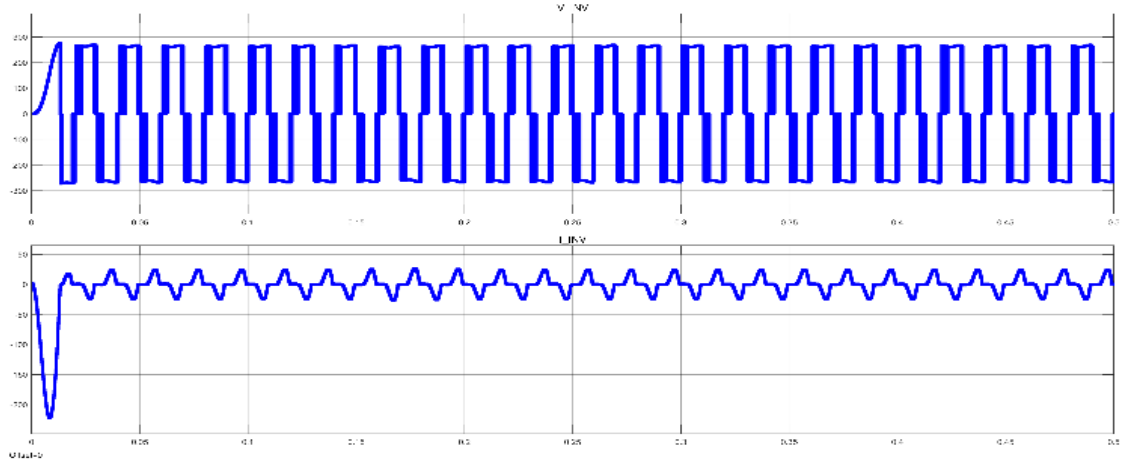

Fig. 5. Phase voltage (three levels) and current waveform of the inverter output

6. Results and Discussions

This section covers the results of the simulations that were run using the suggested model in the MATLAB environment as shown in Figure 6, Figure 7 and Figure 8.

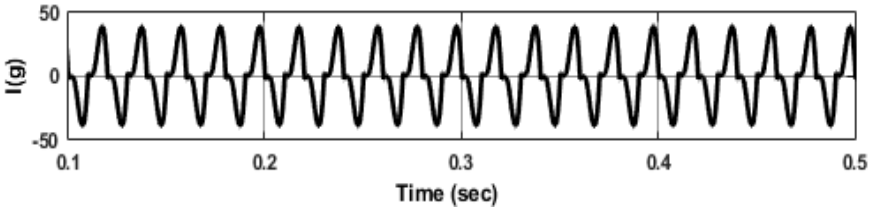

Fig. 6. Three level inverters inject a waveform of grid current

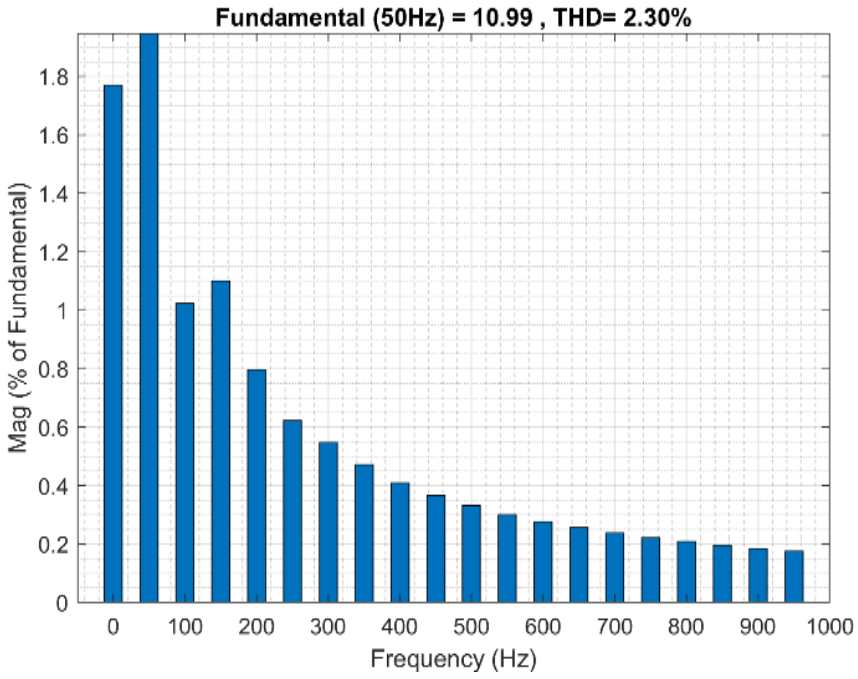

Fig. 7. Graphical representation of fundamental frequency and THD

In this case, a reduction of less than 5% in total harmonic distortion (THD) (see Figure 6) has improved the power system's overall efficiency.

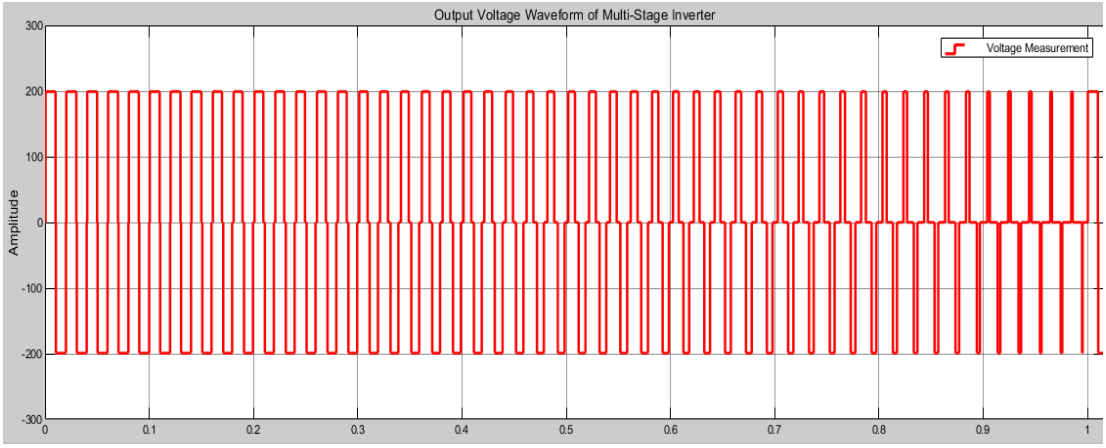

Fig. 8. Simulation characteristics of multi stage inverter

7. Conclusion

In this research paper, a three level H-bridge inverter model and simulation for a single-phase grid-connected solar PV system are described. The proper values of LCL parameters are selected to obtain the best performance of LCL filter. Synchronization of grid frequency and inverter frequency is carried out. This is done by adopting a proper control strategy. The proposed inverter employs a unipolar PWM switching signal scheme to activate its switches. Variations in PV output led to fluctuations in both boost and grid current. Hence, we can deduce that the proposed inverter demonstrates effective responsiveness to environmental changes, a critical aspect for the system's reliable operation. Moreover, the harmonics present in the grid current also shift in accordance with irradiance alterations. When irradiance levels rise, the percentage of Total Harmonic Distortion (%THD) in the grid current decreases. Consequently, during periods of increased irradiance, we can deliver superior-quality power to the grid. Additionally, we obtained a THD reduction of under 5% (Figure 6), which means that the power system's overall efficiency has increased.

References

[1] Samarth, Monali P., and Sumant G. Kadwane. "Single phase grid connected reduced switched multilevel inverter for photovoltaic system." In *2015 IEEE Power, Communication and Information Technology Conference (PCITC)*, pp. 136-141. IEEE, 2015. https://doi.org/10.1109/PCITC.2015.7438148

[2] Aryal, Amit, Ali Hellany, Jamal Rizk, and M. Nagrial. "Residential grid connected solar inverter using fuzzy logic DC-DC Converter." In *2016 International Conference on Sustainable Energy Engineering and Application (ICSEEA)*, pp. 12-16. IEEE, 2016. https://doi.org/10.1109/ICSEEA.2016.7873560

[3] Selvaraj, Jeyraj, and Nasrudin A. Rahim. "Multilevel inverter for grid-connected PV system employing digital PI controller." *IEEE Transactions on Industrial Electronics* 56, no. 1 (2008): 149-158. https://doi.org/10.1109/TIE.2008.928116

[4] Rai, Anil K., N. D. Kaushika, Bhupal Singh, and Niti Agarwal. "Simulation model of ANN based maximum power point tracking controller for solar PV system." *Solar Energy Materials and Solar Cells* 95, no. 2 (2011): 773-778. https://doi.org/10.1016/j.solmat.2010.10.022

[5] Kobayashi, Kenji, Ichiro Takano, and Yoshio Sawada. "A study of a two stage maximum power point tracking control of a photovoltaic system under partially shaded insolation conditions." *Solar Energy Materials and Solar Cells* 90, no. 18-19 (2006): 2975-2988. https://doi.org/10.1016/j.solmat.2006.06.050

[6] Wasynczuk, O. "Modeling and dynamic performance of a line-commutated photovoltaic inverter system." *IEEE Transactions on Energy Conversion* 4, no. 3 (1989): 337-343. https://doi.org/10.1109/60.43233

[7] Salas, Vicente, Emilio Olías, A. Barrado, and A. Lazaro. "Review of the maximum power point tracking algorithms for stand-alone photovoltaic systems." *Solar Energy Materials and Solar Cells* 90, no. 11 (2006): 1555-1578. https://doi.org/10.1016/j.solmat.2005.10.023

[8] Kumar, Varjana Hemant, Pakki Pavan Kumar, and Ramnarayan Patel. "Comparison of dynamic performance of solar PV fed BLDC motor drive with P&O and I. - MPPT Algorithm" *Helix* 9, no. 6 (2019): 5889-5894. https://doi.org/10.29042/2019-5889-5894

[9] Hema Chander, Allamsetty, and Lalit Kumar. "MIC for reliable and efficient harvesting of solar energy." *IET Power Electronics* 12, no. 2 (2019): 267-275. https://doi.org/10.1049/iet-pel.2018.5079

[10] Yadav, Nupur, and D. K. Sambariya. "Analysis and integration of nine level cascaded H-bridge multilevel inverter configuration in a photovoltaic system." In *2018 9th International Conference on Computing, Communication and Networking Technologies (ICCCNT)*, pp. 1-7. IEEE, 2018. https://doi.org/10.1109/ICCCNT.2018.8494046

[11] Bana, Prabhat Ranjan, Kaibalya Prasad Panda, Sanjeevikumar Padmanaban, Lucian Mihet-Popa, Gayadhar Panda, and Jianzhong Wu. "Closed-loop control and performance evaluation of reduced part count multilevel inverter interfacing grid-connected PV system." *IEEE Access* 8 (2020): 75691-75701. https://doi.org/10.1109/ACCESS.2020.2987620

[12] Maurya, Arun Kumar, Anil Kumar Rai, and Hemant Ahuja. "Comparative Analysis of Different MPPT Algorithms for Roof-Top Solar PV System." In *2022 International Conference on Automation, Computing and Renewable Systems (ICACRS)*, pp. 1412-1417. IEEE, 2022. https://doi.org/10.1109/ICACRS55517.2022.10028987

[13] Saafie, Nabilah, Suriati Sufian, Farah Amelia Shahirah Roslan, and Muhamad Irfan Khan. "Optimization of Synthesizing Conditions for MXene (Ti_3C_2) Photocatalyst: Effect of LiF: Ti_3AlC_2 Mass Ratio." *Journal of Advanced Research in Applied Sciences and Engineering Technology* 47, no. 2 (2024): 183-192. https://doi.org/10.37934/araset.47.2.183192

[14] Othman, Zakirah, Bavaani Balakrishnan, Mohamad Faizal Ahmad Zaidi, and Wan Ahmad Jaafar Wan Yahaya. "Adoption Strategy for Electrical and Electronics (E&E) Small and Medium-Sized Enterprises (SMEs): Malaysia IR4. 0 Perspective." *Journal of Advanced Research in Applied Sciences and Engineering Technology* 28, no. 3 (2022): 27-38. https://doi.org/10.37934/araset.28.3.2738

[15] Wagiman, Abdullah, Chan Jun Wei, Ee Min Ci, Martin Ling Teck Seng, Mahmod Abd Hakim Mohamad, and Zamri Noranai. "Design and Performance Evaluation of Hybrid Photovoltaic Thermal Solar Dehydrator." *Journal of Advanced Research in Applied Sciences and Engineering Technology* 28, no. 2 (2022): 181-189. https://doi.org/10.37934/araset.28.2.181189